

Nanocrystalline Aluminum Oxide Coating Fiber Optic Vapour Sensors†

B. RENGANATHAN^{1,*}, D. SASTIKUMAR², R. SRINIVASAN³, A. CHANDRA BOSE² and A.R. GANESAN¹

¹Department of Physics, Indian Institute of Technology Madras, Chennai-600 036, India

²Department of Physics, National Institute of Technology, Tiruchirappalli-620 015, India

³Department of Physics, P.S.R. Engineering College, Sivakasi-626 140, India

*Corresponding author: Fax: +91 44 22574852; E-mail: b.renga79@gmail.com

AJC-12879

Fiber optic sensor based on cladding modification has been developed for detecting various gas emissions such as ammonia, methanol and ethanol. The change in the refractive index of the cladding and the phenomena of evanescent wave absorption forms the underlying principle. The as-prepared aluminum oxide annealed at 1200 °C was used as a gas sensing material. The spectral characteristics of the gas sensor was studied for different concentrations (0-500 ppm) of gases. The sensor exhibits a linear variation in the output light intensity with the concentration. The light intensity as a function of gas concentration exhibits a linear increase for ammonia, ethanol and methanol as-prepared Al₂O₃. However, 1200 °C annealed Al₂O₃ shows decreased sensitivity for methanol gas. The enhanced gas sensitivity and selectivity of the sensor is discussed. The time response characteristics of the sensor are also reported.

Key Words: Annealed Al₂O₃, Ammonia, Ethanol, Methanol gases, Cladding modification, Fiber optic sensor, Gas selectivity.

INTRODUCTION

Aluminum oxide (alumina) is a well known material commercially used for diverse applications such as fabrication of heat-resistant components, high temperature insulating materials for furnaces, electronic insulator, bulk substrate in solid state electrochemical sensor and optical materials in lasers¹⁻³. Recently, alumina has been explored for gas sensing applications. Nanoporous (45-22 nm diameter) alumina films have been examined for NH₃ gas sensing at room temperature. The sensor exhibits good gas sensitivity over these range^{4,5}.

Alumina doped ZnO and barium stannate have been studied as gas sensing materials which exhibits enhanced sensitivity for ethanol^{4,6-11}, CO and H₂¹², respectively. Alumina acts as an adsorption promoter of oxygen and enhances the detection of gases¹³.

A fiber optic sensor is investigated in order to improve the sensitivity, selectivity even in the ambient room temperature. The advantages claimed by the optical fiber sensor over the conventional sensors are immunity to electromagnetic radiation, low cost, small size, high sensitivity and miniaturization¹⁴. The gas sensing mechanism and the underlying principle is based on cladding modification methodology. The enhancement in gas sensing adsorption is achieved by removing a small portion of clad in the optical fiber and

covering with the active gas sensing material. The intensity of the light passing through the fiber is modified when the refractive index of the sensing medium varies with respect to the extent of gas interaction. When the refractive index of the modified cladding is greater than the core, the light rays passing through the fiber would undergo partial reflections at the core/modified-cladding interface, leading to loss of power¹⁵. On the other hand, the refractive index of the modified cladding region is lower than the core, the reflections will increase and the power loss will be diminished. In this work, gas sensing properties of a clad modified optical fiber with aluminum oxide is studied with ammonia, methanol and ethanol gases at room temperature. The time response of the sensor is reported.

EXPERIMENTAL

The experimental setup of the optical fiber sensor is shown in Fig. 1. A white light source (Model SL1, StellarNet Inc., USA with wavelength range from 100 to 2000 nm) and a miniature fiber optic spectrometer (EPP-2000, Stellar Net, USA, having spectral range of 100 to 1100 nm) were used as source and detector. The heart of the sensor was a multimode step index optical fiber having a diameter of 750 μm and a numerical aperture of 0.51. The refractive indices of the core and the cladding are 1.492 and 1.402, respectively. The gas

†International Conference on Nanoscience & Nanotechnology, (ICONN 2013), 18-20 March 2013, SRM University, Kattankulathur, Chennai, India

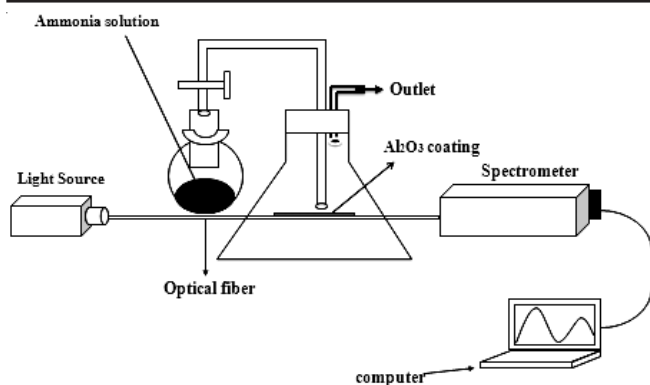


Fig. 1. Schematic diagram of a fiber optic gas sensor

sensing region of about 3 cm was obtained by completely removing the clad part with the careful use of a razor without affecting the core of the fiber. This sensing region was polished to have uniformity and monitored by optical microscope (Macscope, India).

The nanocrystalline Al_2O_3 was mixed with isopropyl alcohol to form a paste and coated on the sensing region by dip coating method. The thickness of the coating was 25 μ . After the coated fiber was dried at room temperature, the sensing part of the fiber was inserted into the gas chamber. Ammonia, methanol and ethanol prepared in different ppm levels (0-500 ppm) were passed into the chamber and the intensity variations were recorded using the spectrometer interfaced with a personal computer. A settling time of 10 min was given after changing the concentrations of ammonia, methanol and ethanol before making measurements for each case. The sensor measurements were carried out at 24 $^\circ\text{C}$.

Synthesis, characterization and gas sensing characteristics of Al_2O_3 nanocrystalline particles

Synthesis: The 0.1 M solution of aluminum chloride was taken in a round bottom flask fitted with a condenser and then it was hydrolyzed for 72 h. The required amount of ammonia solution was added to the hydrolyzed solution and a precipitate was obtained. This precipitate was washed with water several times. Finally aluminum oxide nanopowder was obtained and this powder was annealed at 1200 $^\circ\text{C}$ for 1 h in air. Crystalline natures of the as-prepared and annealed powders were characterized by X-ray diffraction. The surface morphology of the nanoparticles was studied using SEM.

RESULTS AND DISCUSSION

The powder X-ray diffraction studies on the synthesized nanoparticles were performed with Rigaku diffractometer (Model: Ultima III, Japan) using $\text{CuK}\alpha$ (1.54 \AA) radiation. A beam voltage of 40 kV and a beam current of 30 mA were used. The data were collected in the 2θ range (10-80 $^\circ$) with a continuous scan speed of 0.2 $^\circ/\text{min}$. The morphology of the nanoparticles were studied using a scanning electron microscope (SEM) (Model No.S-3000H, Hitachi, Japan).

Fig. 2 shows X-ray powder diffraction pattern of the as-prepared and annealed aluminum oxide nanoparticles. The diffraction pattern shows a tetragonal phase of the aluminum oxide. The grain size and crystallinity increases with annealing temperature. The Scherer's formula was used for estimating

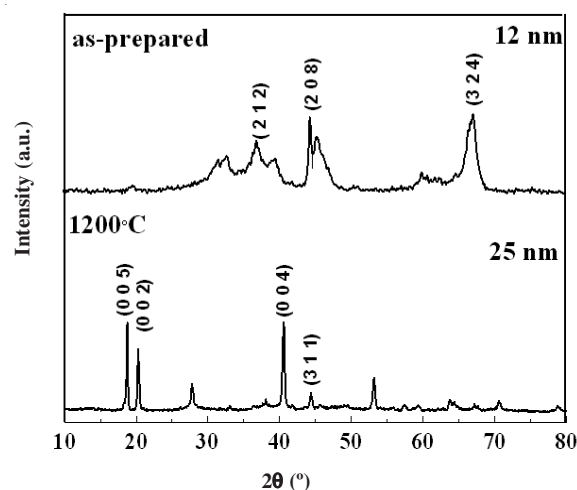
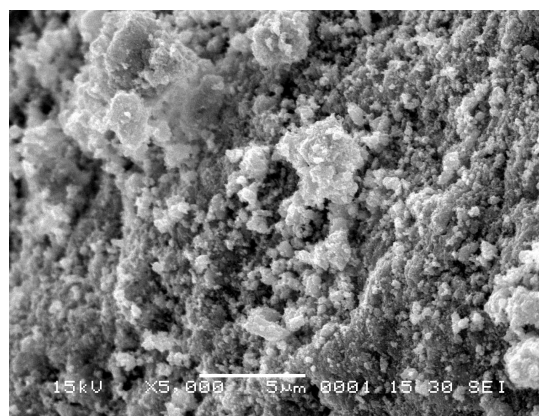


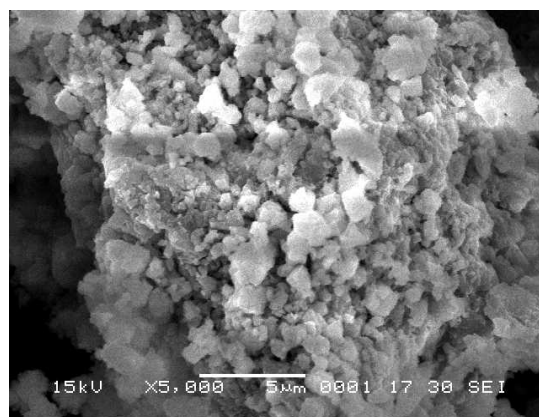
Fig. 2. XRD pattern of the aluminum oxide nanoparticles

the average crystallite size of the aluminum oxide. The estimated sizes of the as-prepared and annealed sample are 12 and 25 nm, respectively.

Figs. 3 and 4 show the SEM micrographs of the as-prepared and annealed samples of aluminum oxide nanoparticles. The different size and shape of the nanoparticles are observed in SEM micrographs of the as-prepared and annealed samples. All the SEM micrographs show the aggregation of many particles which are composed of many primary particles.

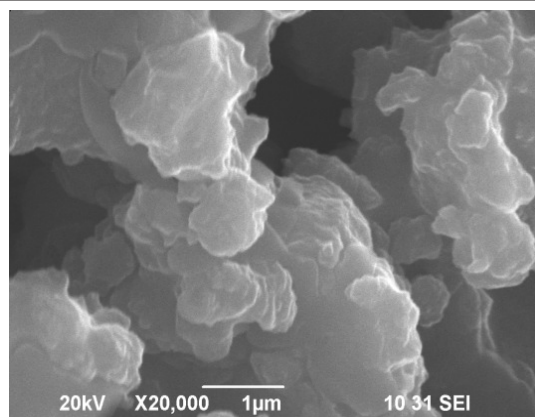


(a)

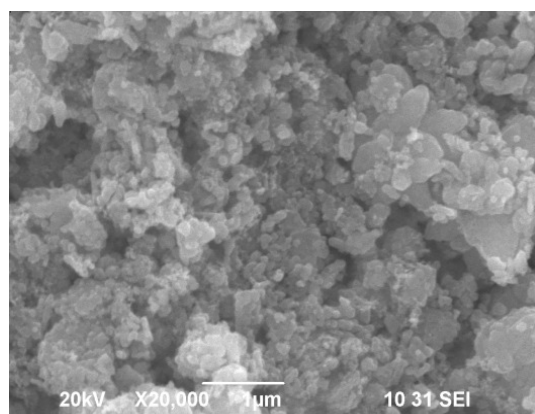


(b)

Fig. 3. SEM micrograph of the (a) as-prepared aluminum oxide nanoparticles; (b) SEM micrograph of the annealed (1200 $^\circ\text{C}$) sample of aluminum oxide nanoparticles



(a)



(b)

Fig. 4. SEM micrograph of the Fiber coating (a) as prepared and (b) annealed (1200 °C) sample of aluminum oxide

Fig. 3(a), (b) and Fig. 4(a),(b) show the SEM micrographs of the as-prepared and annealed (1200 °C) aluminum oxide nanoparticles in the powder form and after coating on the fiber respectively. Different sizes and shapes of nanoparticles are observed. The SEM micrographs show the aggregation of particles which are composed of many primary particles.

Fig. 5(a-c) and Fig. 6(a-c) shows the output spectral characteristics of as-prepared and annealed Al_2O_3 samples exposed to various concentrations ammonia, methanol and ethanol respectively. The spectra exhibit three peaks around 690, 767 and 949 nm. The peak intensity increases for all gases. The annealed samples show lesser variations in peak intensity compared to as prepared sample.

Gas sensitivity and selectivity: Fig. 7(a-c) give the plot between the spectral peak intensity (690 nm) and vapour pressure of ammonia, methanol and ethanol gases for as-prepared and annealed samples. The gas sensitivity is found to be higher for as-prepared sample with ethanol gas ($55 \times 10^{-3}/\text{kPa}$) compared to all other gases and samples. It is about 9 and 29 ($10^{-3}/\text{kPa}$) for ammonia and methanol for as prepared. For the annealed samples the values were 7, 11 and 25 ($10^{-3}/\text{kPa}$) for ammonia, methanol and ethanol respectively.

Though, the as prepared sample exhibits higher gas sensitivity for ethanol, the spectral characteristics are same for all gases (Table-1). Hence, the gas selectivity may be represented in terms of highest gas sensitivity. Thus, Al_2O_3 is best suitable for ethanol detection.

Absorption characteristics of the Al_2O_3 annealed at 1200 °C were studied using spectrophotometer (Model UV-1700, Shimadzu, Japan) under air, ammonia and methanol environ-

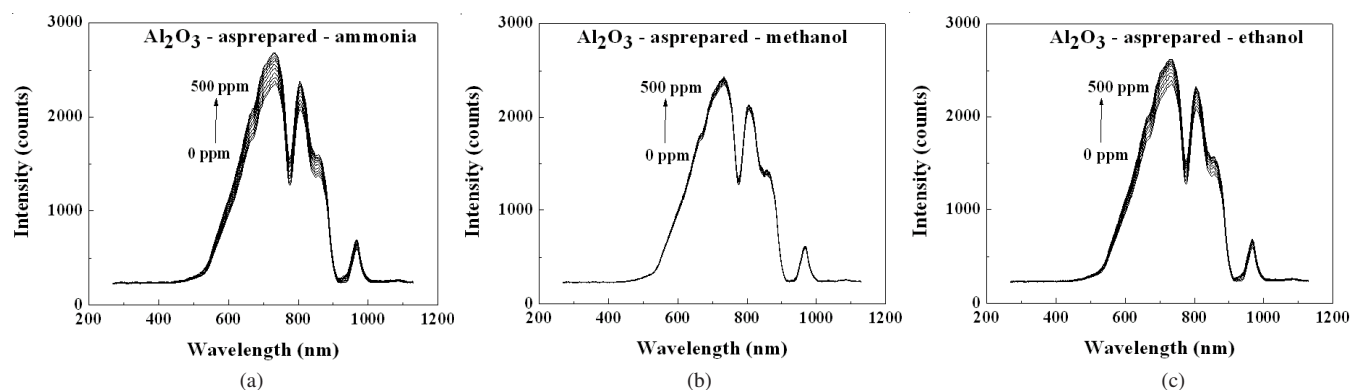


Fig. 5. Spectral response of the sensor with as-prepared Al_2O_3 for various concentrations of (a) ammonia, (b) methanol and (c) ethanol

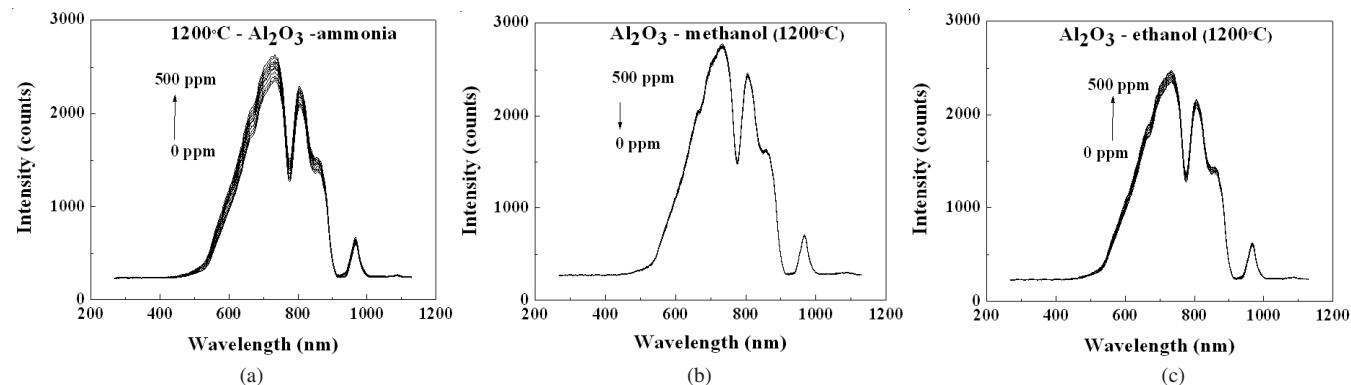


Fig. 6. Spectral response of the sensor with annealed (1200 °C) Al_2O_3 for various concentrations of (a) ammonia (b) methanol and (c) ethanol

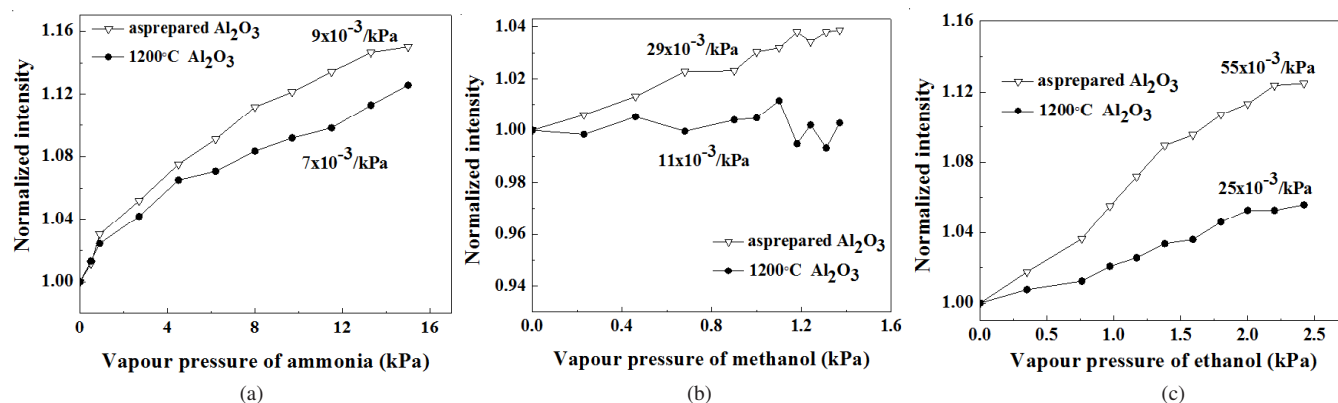


Fig. 7. Plot between peak intensity and various concentrations of (a) ammonia (b) methanol and (c) ethanol in Al₂O₃

TABLE-1 GAS SENSITIVITY OF Al ₂ O ₃ FOR VARIOUS GASES				
Vapours	Gas sensitivity (10 ⁻³ /kPa)			
	As prepared		Annealed at 1200 °C	
Ammonia	9	↑	7	↑
Methanol	29	↑	11	↓
Ethanol	55	↑	25	↑

ments for comparing the proposed model by stimulating the experimental condition for the sample. The annealed Al₂O₃ was coated (around middle portion) on the inside surface of one of the sides of the cuvette and a small amount of solution (about 2 mL) was taken at the bottom of the cuvette for producing a vapour. The coating did not make a contact with the solution. Another similar cuvette with the same amount of solution was taken without any coating for a reference. The open ends of the cuvettes were closed with Teflon lids and the solutions were allowed to vapourize for 10 min.

The absorption characteristics of Al₂O₃ annealed at 1200 °C were also studied by using water alone. The results showed that the spectrum is similar to that of air and its intensity remained almost unchanged with water. This corresponds to an output intensity spectrum obtained when the sensor is not exposed to the gas (and can be taken as a reference value). When the gas is present, the evanescent wave absorption may be higher or lower than the reference value. In the case of methanol, the output light intensity decreases with the increase in the concentration. It indicates that the magnitude of evanescent wave absorption is higher than the air environment. In the case of ammonia, the magnitude of absorption is lower than the air, which results in the increase in the sensor output. It is seen that the light absorption is higher for methanol and lower for ammonia (Fig. 8) compared to the air. These imply that the increase or decrease of the sensor output with methanol or ammonia with the concentration is due to evanescent wave absorption.

Time response characteristics: Fig. 9 shows the time response characteristic for the chamber to reach 500 ppm of ammonia after the vapour has been let in, which shows a good reversibility. The response time was calculated by observing the time duration the sensor signal (at 690 nm) took for raising from 10 to 90 % of the maximum and for recovery time, the intensity fall from 90 to 10 % of the maximum. The response time and recovery time were found to be about 41 and 39 min, respectively.

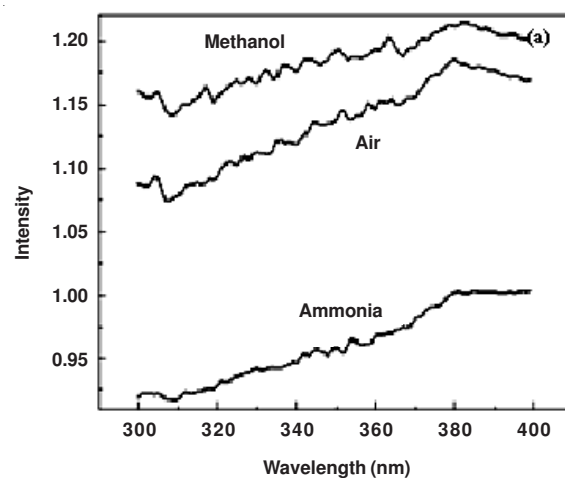


Fig. 8. Absorption spectra of annealed Al₂O₃ (1200 °C) in methanol, air and ammonia environments

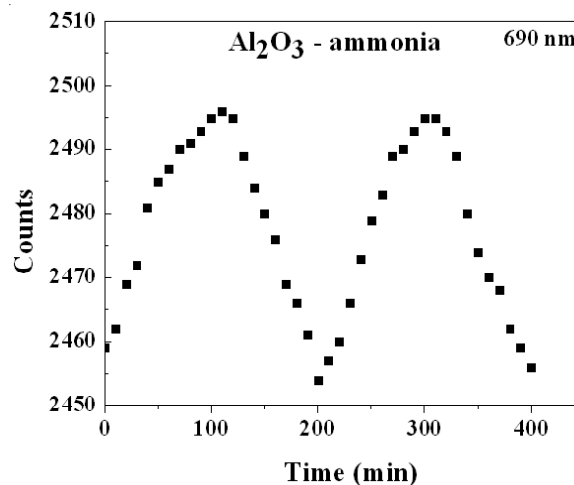


Fig. 9. Time response of the sensor for Al₂O₃ with ammonia gas

Conclusion

The spectral characteristics of the fiber optic sensor with Al₂O₃ coated modified clad were studied for different concentrations of ammonia, methanol and ethanol (0-500 ppm). The sensor showed increase in the spectral intensity for all gases and samples (as prepared and annealed at 1200 °C). The proposed fiber optic gas sensor based on annealed Al₂O₃ as sensing medium exhibited good response for the gases at room temperature, especially best suitable for ethanol detection. The

as prepared sample exhibited good response for ethanol (55×10^{-3} /kPa). The sensor showed good gas selectivity for the ethanol, methanol and ammonia gases.

REFERENCES

1. F.J. Arregui, I.R. Matias, K.L. Cooper and R.O. Claus, IEEE, 0-7803-7289, pp. 443-446 (2002).
2. R.H. French, H. Mullejans and D.J. Jones, *J. Am. Ceram. Soc.*, **81**, 2549 (1998).
3. N. Coowanitwong, C.Y. Wu, M. Cai, M. Ruthkosky, J. Rogers, L. Feng, S. Watano and T. Yoshida, *J. Nanopart. Res.*, **5**, 247 (2003).
4. O.K. Varghese, D. Gong, W.R. Dreschel, K.G. Ong and C.A. Grimes, *Sens. Actuators B*, **94**, 27 (2003).
5. N.D. Hoa, N.V. Quy, Y. Cho and D. Kim, *Sens. Actuators B*, **127**, 447 (2007).
6. R.A. Gerlitz, K.D. Benkstein, D.L. Lahr, J.L. Hertz, C.B. Montgomery, J.E. Bonevich, S. Semancik and M.J. Tarlov, *Sens. Actuators B*, **136**, 257 (2009).
7. N. Han, P. Deng, J. Chen, L. Chai, H. Gao and Y. Chen, *Sens. Actuators B*, **144**, 267 (2010).
8. M.H. Mamat, M.Z. Sahdan, Z. Khusaimi, A.Z. Ahmed, S. Abdullah and M. Rusop, *Opt. Mater.*, **32**, 696 (2010).
9. J.H. Lee and B.O. Park, *Mater. Sci. Eng.*, **106**, 242 (2004).
10. M. Suche, S. Christoulakis, N. Katsaraakis, T. Kitsopoulos and G. Kiriakidi, *Thin Solid Films*, **515**, 6562 (2007).
11. L.M. Li, Z.F. Du and T.H. Wang, *Sens. Actuators B*, **147**, 165 (2010).
12. I. Kocemba, M.W. Jedrzejewska, A. Szychowska, J. Rynkowski and M. Glowka, *Sens. Actuators B*, **121**, 401 (2007).
13. D.R. Patil, L.A. Patil and D.P. Amalnerkar, *Bull. Mater. Sci.*, **30**, 553 (2007).
14. B. Renganathan, D. Sastikumar, G. Gobi, N.R. Yogamalar and A.C. Bose, *Sens. Actuators B*, **156**, 263 (2011).
15. J.P. Hernandez, J. Alberro, E. Llobet, X. Correig, I.R. Matias, F.J. Arregui and E. Palomares, *Sens. Actuators B*, **143**, 103 (2009).